Measurements and models of the atmospheric Ar/N_2 ratio

Mark Battle,[1] Michael Bender,[2] Melissa B. Hendricks,[2] David T. Ho,[3] Robert Mika,[2] Galen McKinley,[4,7] Song-Miao Fan,[5] Tegan Blaine,[6] and Ralph F. Keeling[6]

Received 26 March 2003; revised 8 May 2003; accepted 10 June 2003; published 2 August 2003.

[1] The Ar/N_2 ratio of air measured at 6 globally distributed sites shows annual cycles with amplitudes of 12 to 37 parts in 10^6. Summertime maxima reflect the atmospheric Ar enrichment driven by seasonal warming and degassing of the oceans. Paired models of air-sea heat fluxes and atmospheric tracer transport predict seasonal cycles in the Ar/N_2 ratio that agree with observations, within uncertainties. *INDEX TERMS:* 0312 Atmospheric Composition and Structure: Air/sea constituent fluxes (3339, 4504); 0368 Atmospheric Composition and Structure: Troposphere—constituent transport and chemistry; 0394 Atmospheric Composition and Structure: Instruments and techniques; 3319 Meteorology and Atmospheric Dynamics: General circulation. **Citation:** Battle, M., M. Bender, M. B. Hendricks, D. T. Ho, R. Mika, G. McKinley, S.-M. Fan, T. Blaine, and R. F. Keeling, Measurements and models of the atmospheric Ar/N_2 ratio, *Geophys. Res. Lett.*, *30*(15), 1786, doi:10.1029/2003GL017411, 2003.

[2] Numerical models of oceanic and atmospheric circulation represent our understanding of the physics of these interacting systems. These models in turn contribute to our understanding of climate, biogeochemical processes, and anthropogenic perturbations of the carbon cycle. Here we test aspects of oceanic and atmospheric models by reporting and interpreting measurements of the variations in the Ar/N_2 ratio of air. This newly measured property [*Langenfelds*, 2002] has the potential to uniquely test model calculations of upper-ocean heat fluxes and atmospheric transport.

[3] The Ar/N_2 ratio of air varies because seasonal warming and cooling of the upper ocean changes gas solubilities and drives air-sea fluxes. While all gases leave seawater as it warms, the atmospheric Ar/N_2 ratio over this warming water increases because Ar is more soluble than N_2 [*Weiss*, 1970]. Warming of seawater results from energy transfer (sensible, latent and radiative) to the oceans. Air-sea equilibration of gases may lag the input of heat, and occur over times determined by the depth at which heat absorption occurs, and the ventilation time of the heated waters. These times can range from days to months if the heat transfer occurs below the mixed layer [*Keeling et al.*, 1993]. After the air-sea flux of gas has occurred, there will be a further delay before a concentration change is observed. This is due to transport of the Ar/N_2 signal from the flux source regions to variably distant sampling sites. The length of this transport-based delay will depend on the vigor of lateral motion at different altitudes, vertical mixing, and the dynamics of the planetary boundary layer.

[4] Figure 1 shows our measurements of atmospheric Ar/N_2 at 6 remote, globally distributed sites. These measurements were made on dry whole-air samples collected in 2-liter glass flasks. Names and locations of the sites are given in Table 1. Each point in Figure 1 represents the average of two flasks filled at each collection time. We adopt the unit convention used for O_2/N_2 measurements [*Keeling and Shertz*, 1992] and report changes in the Ar/N_2 ratio of the sample (sa) relative to an arbitrary standard (st) in per meg, defined as

$$\delta(\mathrm{Ar/N_2}) \equiv \left(\frac{\mathrm{Ar/N_{2_{sa}}}}{\mathrm{Ar/N_{2_{st}}}} - 1 \right) \times 10^6$$

[5] The samples were analyzed for Ar/N_2 and O_2/N_2 using an isotope-ratio mass spectrometer. $\delta(Ar/N_2)$ was measured in the instrument's normal comparison mode, alternately measuring the Ar/N_2 ratio (mass 40/mass 28) of dry air samples and the dry air standard. Analytic details are presented in the auxiliary material.[1] CO_2 concentrations were also measured in these samples by NOAA/CMDL [*Conway et al.*, 1988]. While our O_2/N_2 measurements began in 1991 [*Bender et al.*, 1995], we initiated our measurements of Ar/N_2 only in early 1999.

[6] To extract an atmospheric signal from our raw measurements, we eliminate all flask pairs whose Ar/N_2 values differ by more than 20 per meg (a 2-σ cut). We then collapse the records for each site into a single year. For each month, we calculate an average value, along with a standard error (reflecting only the scatter of the values averaged within each month). These are the values and error bars presented in Figure 1. We then use the monthly values and their errors to calculate annual averages and cycle amplitudes (simply *max.* − *min.*). Other fitting methods [*Chambers et al.*, 1983;

[1]Department of Physics and Astronomy, Bowdoin College, Brunswick, Maine, USA.
[2]Department of Geosciences, Guyot Hall, Princeton University, Princeton, New Jersey, USA.
[3]Princeton Environmental Institute, Princeton University, Princeton, New Jersey, 08544 USA. Now at Lamont-Doherty Earth Observatory, Columbia University, Palisades, NY 10964, USA.
[4]Department of Earth, Atmospheric and Planetary Sciences, Massachusetts Institute of Technology, Cambridge, Massachusetts, USA.
[5]Atmospheric & Oceanic Sciences Program, Sayre Hall, Princeton University, Princeton, New Jersey, USA.
[6]Scripps Institute of Oceanography, University of California, San Diego, La Jolla, California, USA.
[7]Now at Instituto Nacional de Ecología, Periférico 5000, 4 piso, México, DF 04530, MEXICO.

0094-8276/03/2003GL017411$05.00

[1]Auxiliary material is available at ftp://ftp.agu.org/apend/gl/2003GL017411.

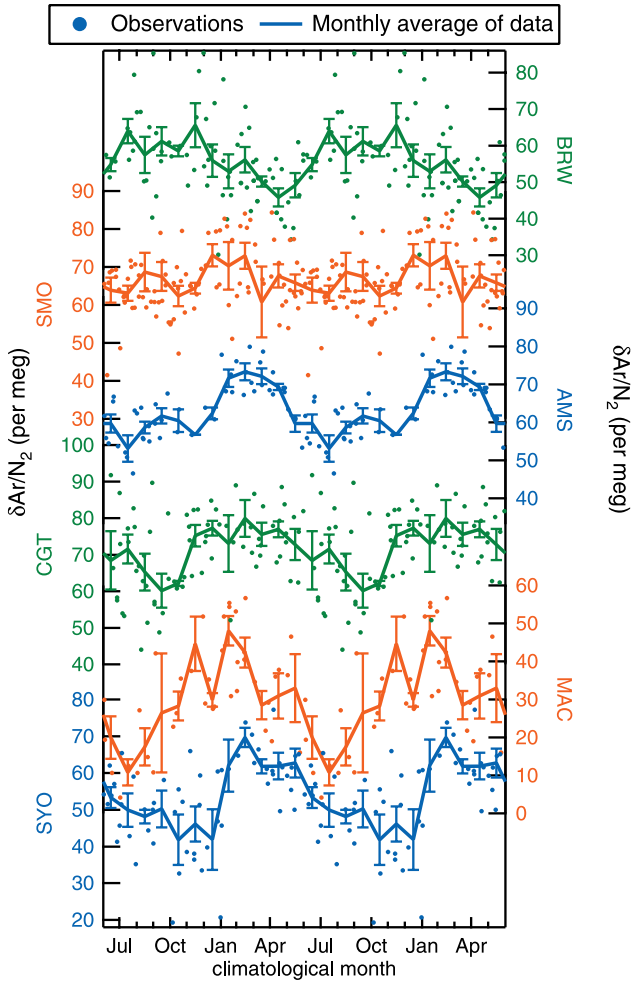

Figure 1. Ar/N_2 measurements (points) of air collected at 6 sites. Bars show standard errors on monthly average values. All records are displayed in a single climatological year. No new information is shown before Jan. 1 or after Dec. 31. Line segments connecting monthly average values simply guide the eye. Complete time series are shown in the online supplement.

Thoning et al. 1989] yield nearly identical values for the amplitudes and phasings of the seasonal cycles. Values are summarized in Table 1. Some error bars are particularly large (e.g. October at Macquarie). These typically occur in months where we have relatively few data, among which is a signficant outlier retained by our objective criteria. During December at Amsterdam Island, we have only one collection, so no error can be calculated.

[7] Each site shows a distinct seasonal cycle. The five Southern Hemisphere sites are in phase with each other, but out of phase with Barrow. As expected, Ar/N_2 is high in the local summer when seawater is warm and gases are relatively insoluble. Seasonality is most pronounced at high latitudes and is stronger in the South than in the North because of the greater areal extent of the oceans.

[8] Some of the scatter in the data reflects real atmospheric change within the month-long period of averaging. Other scatter reflects real interannual variability in the atmospheric seasonal cycle. Model results presented below indicate that any variability of this type is probably due to variability in atmospheric transport (rather than variability in ocean heat fluxes). The remaining scatter in the data is an artifact of sample collection and analysis.

[9] We believe multiple processes are responsible for the scatter in our data during both collection and analysis. Among these processes are limited instrumental precision, fractionation during sample collection and fractionation during transfer of the aliquot from the flask to the ionization chamber of the mass spectrometer. These sources of error are discussed in the auxiliary materials. In brief, we see no evidence for a single process that is primarily responsible for the scatter.

[10] None of our 6 sites shows a statistically signficant trend over the full period of record (slopes are less than 1.2 per meg/yr with an uncertainty of at least 1.3 per meg/yr). This absence of a trend is consistent with a freedom from drift in the standards against which our samples are measured. Our data are too imprecise to resolve any interannual rise in Ar/N_2 associated with long-term ocean warming [*Levitus et al.*, 2000]. We expect this trend in Ar/N_2 to be roughly 0.3 per meg/year.

[11] The annual-mean gradients of Ar/N_2 between sites are also potentially informative, but we expect them to be very small (of order 2 per meg or less, based on the model results presented below). The much larger gradients that we observe (see Table 1) are almost certainly due to collection artifacts. A likely explanation for these apparent gradients is thermal fractionation at the air intake that varies from site to site [*Manning*, 2001]. It is possible that these thermal gradients might be correlated with the season of collection,

Table 1. Sampling Sites and Summary of Results From This Study

	Barrow, Alaska (BRW)	American Samoa (SMO)	Amsterdam Island (AMS)	Cape Grim, Tasmania (CGT)	Macquarie Island (MAC)	Syowa, Antarctica (SYO)
	71°N 157°W	14°S 171°W	38°S 77°E	41°S 145°E	55°S 159°E	69°S 40°E
			Period of Ar/N_2 record considered here (month/year)			
	2/99–2/02	3/99–2/02	3/99–10/01	4/99–2/02	11/98–3/01	2/98–2/01
			Annual mean Ar/N_2			
	56	67	63	72	30	54
			Total number of collections (and number failing 2σ cut) for each station			
	82 (13)	102 (6)	51 (4)	76 (7)	39 (5)	69 (17)
			Seasonal cycle amplitude			
Data	20 ± 7	12 ± 10	20 ± 4	20 ± 7	37 ± 5	28 ± 7
ECMWF/TM2	17	9.5	19.5	22	23	27
ECMWF/GCTM	14	6	16	17	21	16
MIT/GCTM	13.5	9	23	23	29	18

All Ar/N_2 values are given in per meg.

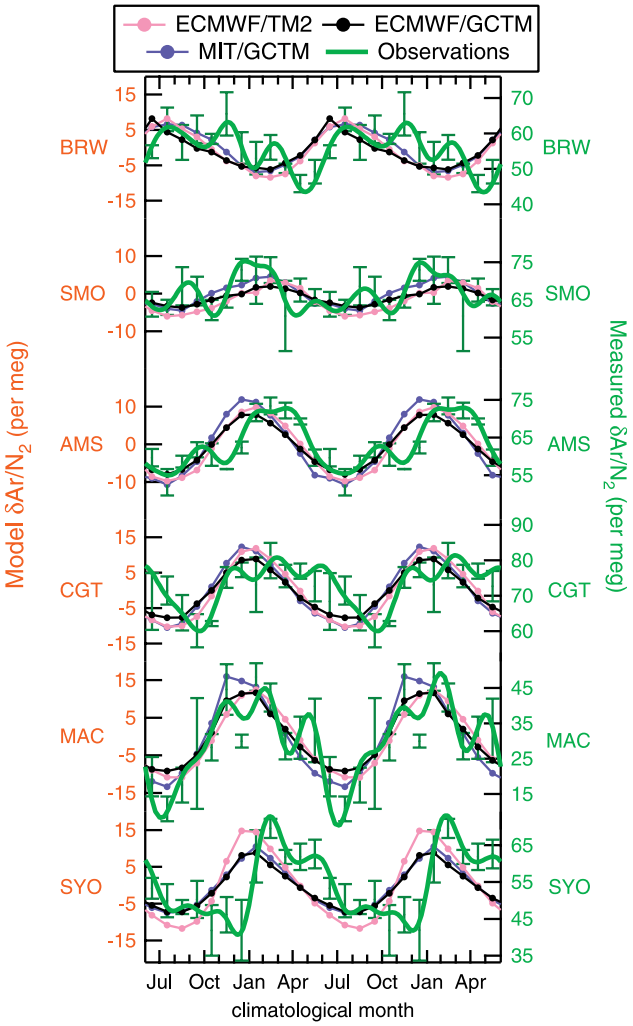

Figure 2. Seasonal cycles of Ar/N_2 predicted by 3 ocean-atmosphere model combinations. Model output is presented as monthly average values (points connected with straight lines). Monthly averaged data (see Figure 1) are also shown (points with error bars) along with a fit [*Thoning et al.*, 1989] to the unbinned data. See text for model descriptions.

thereby biasing our measured seasonal cycle. While this remains a possibility, other aspects of our dataset (discussed in the online material) suggest that the seasonal cycle we see is not biased in this fashion.

[12] We next compare the seasonal cycles we observe with predictions from 3 paired models (Figure 2). Each paired model invokes modeled or observed air-sea heat fluxes to generate time series of sea-air fluxes of Ar and N_2. These sea-air gas fluxes serve as boundary conditions for an atmospheric tracer transport model that predicts Ar/N_2 at our observing sites as a function of time.

[13] The first model pair (ECMWF/TM2) combines air-sea gas fluxes calculated directly from heat fluxes, with the TM2 atmospheric tracer transport model [*Heimann*, 1995]. In this model pair, the monthly air-sea gas fluxes were generated using climatological ECMWF air-sea heat fluxes [*Gibson et al.*, 1997]. The annual mean at every grid point was removed initially from the monthly heat flux fields in order to leave only the seasonal cycle. Using an SST monthly data set [*Shea et al.*, 1992] masked for land and ice and assuming constant salinity, we calculated the derivative of the Weiss solubility relationship [*Weiss*, 1970] with respect to temperature at a given gridpoint and time. This value was then used with the ECMWF heat fluxes to calculate gas fluxes following the method of *Keeling et al.* [1993] (eq. 19). The air-sea gas fluxes were then regridded to the resolution of TM2 and used as a boundary condition for a 4-year run of TM2. The monthly mean output at each of our stations was saved from the fourth year of the run.

[14] The second model pair (ECMWF/GCTM) uses exactly the same ECMWF-derived gas fluxes as the first pair, but distributes these fluxes using the GCTM atmospheric tracer transport model [*Mahlman and Moxim*, 1978; *Levy et al.*, 1982].

[15] The third model pair (MIT/GCTM) uses gas fluxes derived from the heat fluxes of the MIT ocean general circulation model [*McKinley et al.*, 2003] and distributes them using GCTM. The total model heat flux is the sum of the model forcing term and the heat flux implied by the relaxation of sea surface temperature (SST) to the climatology [*Reynolds and Smith*, 1994]. The model forcing is the sum of NCEP variability for 1980–1998 and the COADS long-term mean. These total heat fluxes, masked by sea ice, along with model-predicted SST and sea surface salinity are converted to air-sea gas fluxes at 10-day resolution for the period 1980–1998 using the same relationship employed for ECMWF/TM2 [*Keeling et al.*, 1993]. Like the ECMWF heat fluxes, the total MIT model heat flux has a non-zero global mean, causing net fluxes of Ar and N_2 to the atmosphere. The resulting trend in Ar/N_2 was removed before comparison with the observations.

[16] The MIT/GCTM model pair generates air-sea gas fluxes that vary interannually, but distributes them with a stationary atmospheric tracer-transport model. Thus, the interannual variability in the modelled monthly mean Ar/N_2 values reflects only part of true natural variability. We find that monthly mean predictions by MIT/GCTM vary by less than 1 per meg from year to year. This result suggests that variability in oceanic heat fluxes does not make a significant contribution to interannual variability of Ar/N_2.

[17] We treat the model output and data as similarly as possible. For the MIT model, we calculate monthly mean values for each month of each year, and then group the years together into a single virtual year, averaging all years of each particular month. For all 3 model pairs, the monthly means are shown in Figure 2.

[18] In general, the models agree with each other and with the observations, matching the amplitudes of the measured seasonal cycles at nearly all sites within 1σ (see Table 1). While our data are not yet precise enough to separately assess the oceanic and atmospheric components of the models, the simplest interpretation is that air-sea fluxes of inert gases are indeed closely tied to heat fluxes in the upper ocean, and that model descriptions of vertical and lateral atmospheric transport of a tracer with a seasonal ocean source are generally correct.

[19] The most obvious data-model discrepancy is in the phasing of the seasonal cycle. The models lead the observations at 5 of the 6 stations by up to 2 months (at Amsterdam Island and Syowa). One indisputable source of this discrepancy is the assumption, common to our

models, of instantaneous equilibration between the ocean and the atmosphere. Until the ocean models include Ar and N_2 as active tracers, we cannot use data-model phase information to quantitatively assess lateral or vertical transport in the atmospheric models.

[20] The most obvious model-model discrepancies are in the amplitudes of the cycles at Syowa and Macquarie. At Syowa, comparing ECMWF/TM2 with ECMWF/GCTM shows that differences in transport between TM2 and GCTM are responsible. There are indications from measurement of atmospheric ^{222}Rn and O_2/N_2 that atmospheric transport models may not correctly capture the seasonality of transport over Antarctica [*Heimann et al.*, 1990; *Stephens*, 1999]. In contrast, at Macquarie the different amplitudes are due to different air-sea gas fluxes. Since the SST relaxation term in the MIT model is small at high latitudes, differences between ECMWF and NCEP heat fluxes probably explain the discrepancy at Macquarie. Also noteworthy is the fact that the amplitude of the Cape Grim cycle predicted by ECMWF/GCTM is ~6 per meg less than the predictions of the other model pairs. This discrepancy shows that the ECMWF/TM2-MIT/GCTM agreement is coincidental, and that the present uncertainties in heat fluxes and atmospheric transport have consequences of comparable magnitude.

[21] Independent of any models, Ar/N_2 directly gives the size of the solubility-driven O_2/N_2 cycle. Like Ar/N_2, O_2/N_2 varies seasonally due to temperature-driven solubility changes. Unlike Ar/N_2, the O_2/N_2 cycle also has a biological component of great interest [*Keeling and Shertz*, 1992; *Keeling et al.*, 1993; *Bender et al.*, 1998]. Ar/N_2 measurements provide the first empirical method for separating the biological and solubility parts of the O_2/N_2 cycle. Simply accounting for the relative solubilities of O_2 and Ar [*Weiss*, 1970] allows us to convert from Ar/N_2 amplitudes to O_2/N_2 amplitudes. These calculations show that solubility changes alone account for 13 ± 4 to $34 \pm 5\%$ of the total O_2/N_2 cycle measured from these flasks at Barrow and Macquarie respectively.

[22] We look forward to improvements in both data and interpretation. The fact that some stations show less scatter than others indicates room for refinements in sampling protocol. Longer records and more sampling stations will improve climatologies and provide more insight into the site-to-site artifacts in our present dataset. While we find general agreement between observations and predictions of the seasonal Ar/N_2 cycle, the predicted Ar/N_2 variations do differ significantly between competing models. Improved Ar/N_2 records will enable assesment of which models give the best simulations of atmospheric transport. Additional sampling sites in continental interiors will allow us to quantify the diminution in the seasonal cycle as air masses move over the land. This will help to assess the exchange rates of air between the open oceans and continental interiors. We hope also to eventually resolve the signals related to interannual variability in oceanic and atmospheric processes.

[23] **Acknowledgments.** We thank the staffs of the observatories for their careful collections and Pieter Tans for comments. Cape Grim and Macquarie data are collected under the umbrella of the CSIRO Atmospheric Research Program (in collaboration with R. J. Francey and R. L. Langenfelds) supported by the Australian Bureau of Meteorology and the Australian Antarctic Division. Our flasks are also used in an ongoing collaboration with NOAA/CMDL-CCG. Grants from the National Science Foundation, the NOAA Global Change Research Program, The Princeton/BP Amoco Carbon Mitigation Initiative, Ford Research Lab, the NASA Earth System Science Fellowship Program and the National Defense Science and Engineering Graduate Fellowship Program supported this work.

References

Bender, M. L., P. P. Tans, J. T. Ellis, J. Orchardo, and K. Habfast, A high precision isotope ratio mass spectrometry method for measuring the O_2/N_2 ratio of air, *Geochimica et Cosmochimica Acta*, *58*, 4751–4758, 1995.

Bender, M. L., M. Battle, and R. F. Keeling, The O_2 balance of the atmopshere: A tool for studying the fate of fossil-fuel CO_2, *Annual Reviews of Energy and the Environment*, *23*, 207–223, 1998.

Chambers, J. M., W. S. Cleveland, B. Kleiner, and P. A. Tukey, *Graphical Methods for Data Analysis*, The Wadsworth Statistics/Probability Series, Wadsworth International Group, 1983.

Conway, T. J., P. Tans, L. S. Waterman, K. W. Thoning, K. A. Masarie, and R. H. Gammon, Atmospheric carbon dioxide measurements in the remote global troposphere 1981–1984, *Tellus*, *40B*, 81–115, 1988.

Gibson, J., P. Kallberg, S. Uppala, A. Hernandez, A. Nomura, and E. Serrano, Era description, ECMWF re-analysis project report, *Tech. Rep. Ser. I*, 72 pp., European Center for Medium-Range Weather Forecasts, 1997.

Heimann, M., The global atmospheric tracer model TM2, *Tech. Rep. 10*, Deutsches Kimarechenzentrum, Hamburg, Germany, 1995.

Heimann, M., P. Monfray, and G. Polian, Modelling the long-range transport of ^{222}Rn to subantarctic and antarctic areas, *Tellus B*, *41*, 83–99, 1990.

Keeling, R. F., and S. R. Shertz, Seasonal and interannual variations in atmospheric oxygen and implications for the global carbon cycle, *Nature*, *358*, 723–727, 1992.

Keeling, R. F., R. P. Najjar, M. L. Bender, and P. P. Tans, What atmospheric oxygen measurements can tell us about the global carbon cycle, *Global Biogeochemical Cycles*, *7*, 37–67, 1993.

Langenfelds, R. L., Studies of the global carbon cycle using atmospheric oxygen and associated tracers, Ph.D. thesis, University of Tasmania, 2002.

Levitus, S., J. Antonov, T. Boyer, and C. Stephens, Warming of the world ocean, *Science*, *287*, 2225–2229, 2000.

Levy, H., II, J. D. Mahlman, and W. J. Moxim, Tropospheric N_2O variability, *Journal of Geophysical Research*, *87*, 3061–3080, 1982.

Mahlman, J. D., and W. J. Moxim, Tracer simulation using a global general circulation model: Results from a mid-latitude instaneous source experiment, *Journal of Atmospheric Sciences*, *35*, 1340–1374, 1978.

Manning, A. C., Temporal variability of atmospheric oxygen from both continuous measurements and a flask sampling network: Tools for studying the global carbon cycle, Ph.D. thesis, University of California, San Diego, 2001.

McKinley, G. A., M. J. Follows, J. Marshall, and S. Fan, Interannual variability of air-sea O_2 fluxes and the determination of global CO_2 sinks using atmospheric O_2/N_2, *Geophysical Research Letters*, *30*, 1101, 2003.

Reynolds, R., and T. Smith, Improved global sea surface temperature analyses, *Journal of Climate*, *7*, 929–948, 1994.

Shea, D., K. Trenberth, and R. Reynolds, A global monthly sea surface temperature climatology, *Journal of Climate*, *5*, 987–1001, 1992.

Stephens, B. B., Field-based atmospheric oxygen measurements and the ocean carbon cycle, Ph.D. thesis, University of California, San Diego, 1999.

Thoning, K. W., P. P. Tans, and W. D. Komhyr, Atmospheric carbon dioxide at Mauna Loa observatory 2. Analysis of the NOAA GMCC data, 1974–1985, *Journal of Geophysical Research*, *94*, 8549–8565, 1989.

Weiss, R. F., The solubility of nitrogen, oxygen, and argon in water and seawater, *Deep-Sea Research*, *17*, 721–735, 1970.

M. Battle, Department of Physics and Astronomy, Bowdoin College, 8800 College Station, Brunswick, ME 04011, USA. (mbattle@bowdoin.edu)